Proceedings of the Fifth Workshop on
Mathematical Modelling
of Environmental and Life Sciences Problems
Constanţa, Romania, September, 2006, pp. 153–162

A Simulation Study of Electrical Rhythms in a Paced Cardiac Fiber ♮

Daniel Mocanu[*], **Mihaela Morega**[*†] and **Alexandru Morega**[*‡]

November 11, 2008

The cardiac electrical activity is macroscopically manifested as action potentials that travel through atria and ventricles in a synchronized fashion. Cardiac arrhythmias are disorders of the normal electrical rhythm. At high heart rate, the action potential duration follows a long-short-long pattern. This oscillatory electrical rhythm is called alternans and it is believed to be a precursor to the development of severe ventricular arrhythmias. In this computational study we analyze the initiation of alternans in a paced one-dimensional strand of cardiac cells governed by the Beeler-Reuter model. We present results from numerical experiments and a qualitative description of the observed patterns of cardiac activation.

Keywords: cardiac propagation, pacing, alternans, Beeler-Reuter model, cable equation.

1. Introduction

The bioelectric activity of cardiac cells results from the transport processes of ionic species across the membrane through voltage-gated ion channels. The ion channels act as gates that regulate the permeabilities of sodium, potassium and calcium ions. At rest, the cell maintains a constant, negative transmembrane voltage, called the resting potential. However, if a strong enough depolarizing current is passed through the membrane, the cell departs from equilibrium and responds with a sharp change in the transmembrane voltage followed by a return to the resting state. This

[*] Politehnica University Bucharest, Department of Bioengineering and Biotechnology,
[†] e-mail: mihaela@iem.pub.ro
[‡] e-mail: amm@iem.pub.ro
♮ This study was supported by the research grant CEEX 05-D11-25/05.10.05.

rapid course of the transmembrane voltage is called *action potential* (AP). Conduction of AP in the heart occurs by electrotonic mechanisms, in which the local release of stored energy is spent to trigger similar cellular events in adjacent regions [1]. Action potential waves are self-sustaining signals in the sense that they retain their amplitude and shape at the expense of energy provided by the cell metabolism.

During normal sinus rhythm, AP waves are periodically initiated by the pacemaker cells of the sinoatrial node and propagate through atria and ventricles. Cardiac arrhythmias are disorders of either wave initiation or wave propagation. A common cardiac arrhythmia is alternans, which is characterized by a long-short alternation of action potential duration (APD) during rapid pacing [2]. It has been suggested that alternans may be a precursor of more severe cardiac disorders, such as ventricular fibrillation [3]. Alternans can be concordant or discordant. During concordant alternans, APD oscillations are in phase everywhere in the tissue. Discordant alternans are characterized by APD oscillations of opposite phases in distinct spatial regions of the cardiac tissue [4]. The development of alternans is closely related to the restitution property of the cardiac tissue. Restitution is the relationship between the action potential duration (APD) and the diastolic interval (DI), which is the time interval between the end of the preceding AP and the start of the next one [4]. More precisely, by decreasing the DI the APD of a cell shortens. Below a critical value of DI, the cell does not respond with an action potential. Cardiac alternans is produced during high-frequency pacing when the slope of the restitution curve is greater than one [5]. Clinically, the suppression of cardiac alternans is achieved with calcium channel blockers or bretylium, which have been shown to flatten the restitution curve [12]. Alternans is also called a $\{2:2\}$ rhythm, meaning that two stimuli elicit two action potentials of different duration and shape. Increasing the stimulation frequency leads to conduction block and $\{2:1\}$ synchronization, in which the cardiac tissue responds to every other stimulus.

In this computational study we analyze different cardiac electrical rhythms and the initiation of alternans in a paced one-dimensional strand of cardiac cells governed by the *Beeler-Reuter* model [6]. We present results from numerical experiments and a qualitative description of the observed patterns of cardiac activation.

2. Physical Model

Action potential propagation in a one-dimensional strand of ventricular muscle was modeled using the cable equation as in [7]. We assumed that cardiac cells are cylinders that connect to one another, forming a continuous long cylindrical fiber (fig. 1). According to the cable theory [7], any change of current in axial direction must equal the transmembrane current, which is composed of a capacitive current and a ionic current

$$C_m = \frac{\partial V_m}{\partial t} + I_{ion} = \frac{r}{2\rho}\frac{\partial^2 V_m}{\partial x^2}, \tag{1}$$

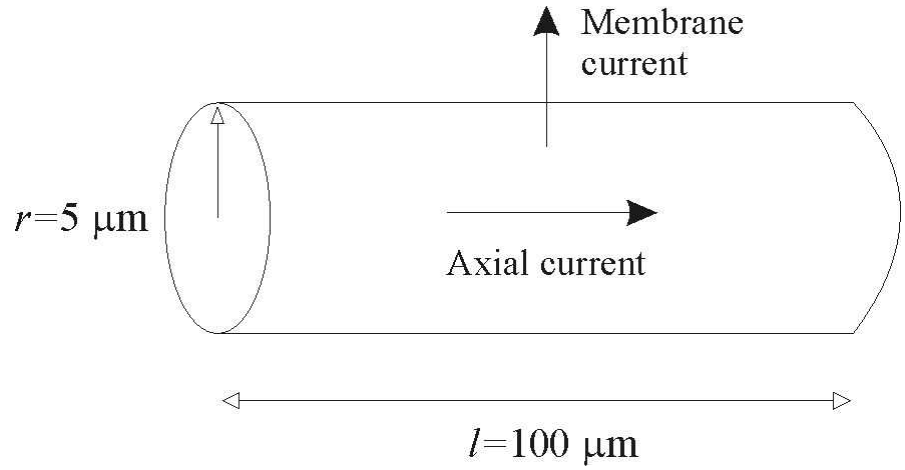

Fig. 1. A cell element in the cable model, with radius $r = 5\,\mu$m and length $l = 100\,\mu$m.

where V_m (mV) is the transmembrane voltage, $C_m = 1\,\mu\text{F/cm}^2$ is the membrane capacitance, $r = 5\,\mu$m is the cardiac cell radius, $\rho = 0.25\,\text{k}\Omega \cdot \text{cm}$ is the intracellular axial resistivity, $L = 7\,$cm is the length of the cable and I_{ion} ($\frac{\mu\text{A}}{\text{cm}^2}$) is the ionic current through the cell membrane, described by the Beeler-Reuter (BR) model of the ventricular cell. Equation (1) was solved to simulate action potential propagation when the cardiac fiber was paced at one end by injecting an axial current I_{stim}, while the other end was electrically sealed

$$\frac{1}{\rho}\frac{\partial Vm}{\partial x}\bigg|_{x=0} = -I_{stim},\ \frac{1}{\rho}\frac{\partial Vm}{\partial x}\bigg|_{x=L} = 0. \tag{2}$$

The initial condition was $V_{\text{m}}(0) = -85\,$mV, which corresponds to the resting potential of the cardiac cell.

The ionic current I_{ion} represents the sum of the current densities corresponding to three ionic species: sodium, calcium and potassium

$$I_{ion} = I_{\text{Na}} + I_{\text{K}} + I_{x_1} + I_S, \tag{3}$$

where I_{Na} is the sodium current, I_K and I_{x_1} are potassium currents and I_S is the calcium current. For the inward sodium current we used the revised formulation of the BR model given in [8]

$$I_{\text{Na}} = G_{\text{Na}} m^3 h\,(V_m - E_{\text{Na}})\,, \tag{4}$$

where $G_{\text{Na}} = 15\,\text{mS/cm}^2$ is the maximal conductance of the Na^+ channels, $E_{\text{Na}} = 40\,$mV is the equilibrium Nernst potential for the Na^+ ions, and m and h are dimensionless gating variables, describing the opening and closing of Na^+ ionic channels. The inward calcium current is given by

$$I_S = G_S f d\,(V_m - E_s)\,, \tag{5}$$

where $G_S = 0.09\,\mathrm{mS/cm^2}$ is the maximal conductance of the Ca^{2+} channels,$E_s(\mathrm{mV}) = -82.13 - 13.0287\ln[Ca]$ is the equilibrium Nernst potential for the Ca^{2+} ions, and f and d are dimensionless gating variables, describing the opening and closing of Ca^{2+} ionic channels. Intracellular Ca^{2+} concentration [Ca] changes according to

$$\frac{\mathrm{d}\,[\mathrm{Ca}]}{\mathrm{d}t} = -10^{-7} I_S + 0.07\left(10^{-7} - [\mathrm{Ca}]\right). \tag{6}$$

The outward potassium current is a function of transmembrane voltage

$$I_{\mathrm{K}} = 1.4\frac{\exp\left[0.04\left(V_m + 85\right)\right] - 1}{\exp\left[0.08\left(V_m + 53\right)\right] + \exp\left[0.04\left(V_m + 53\right)\right]}, \tag{7}$$

and the time-activated outward potassium current has a gating variable x_1

$$I_{x_1} = 0.8 x_1 \frac{\exp\left[0.04\left(V_m + 77\right)\right] - 1}{\exp\left[0.04\left(V_m + 35\right)\right]}. \tag{8}$$

The gating variables m, h, d, f, and x_1 follow the dynamics

$$\frac{\mathrm{d}a}{\mathrm{d}t} = \frac{a_\infty\left(V_m\right) - a}{\tau_a\left(V_m\right)},\ a = \{m, h, d, f, x_1\}. \tag{9}$$

The individual expressions for a_∞ and τ_a can be found in [6].

Thus, the mathematical model consists of seven differential equations, described by (1), (6) and (9), subject to boundary conditions (2) and to the following initial conditions: $V_m(0) = -85\,\mathrm{mV}$, $[\mathrm{Ca}]_{\mathrm{i}}(0) = 3 \cdot 10^{-7}\,\mathrm{M}$, $m(0) = 0.01126$, $h(0) = 0.9871$, $d(0) = 0.003$, $f(0) = 1$, $x_1(0) = 0.0241$. Equation (1) was discretized using the finite difference method in conjunction with the Crank-Nicolson time stepping scheme. The resulting tridiagonal system of linear equations was solved using the Thomas algorithm [9]. The ordinary differential equations (6) and (9) were solved numerically using the forward Euler method [9]. A cable of 7 cm in length was used in all simulations. The grid space was $h = 0.01\,\mathrm{cm}$ and the time step was $k = 0.025\,\mathrm{ms}$. The diffusion coefficient is $D = \frac{r}{2\rho C_m} = 10^{-3}\,\mathrm{cm^2/ms}$, so that the stability criterion $\frac{h^2}{k} > 2D$ is satisfied. In all simulations, the amplitude of the current stimulus was twice the diastolic threshold as measured in our numerical model, $I_{stim} = 70\,\mu\mathrm{A/cm^2}$, and had a duration of 2 ms (typical value used in experiments).

3. Results

Figure 2a shows a typical action potential obtained with the BR model. The numerical method used resulted in an APD of 300 ms and an upstroke velocity of 120 V/s. The conduction velocity along the cable was 65 cm/s. Figures 2b, 2c show the time evolution of the ionic currents. The sharp depolarization of the cell (phase 0) is mainly due to the fast inward Na^+ current (fig. 2b). The brief repolarization, represented by a notch at the end of the upstroke (phase 1), owes to the activation of

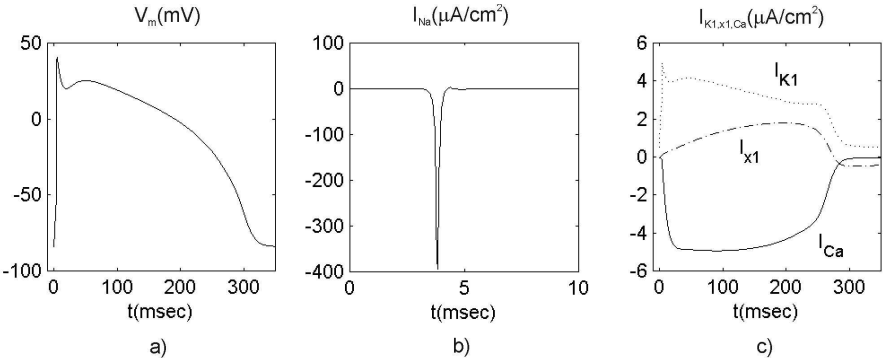

Fig. 2. a) Simulated action potential V_m in the Beeler-Reuter model; b) time variation of the fast inward Na^+ current during an action potential; c) time variation of the K^+ and Ca^{2+} currents during an action potential.

outward currents carried by K^+ ions, while the plateau of the action potential (phase 2) is determined by a balance between the outward K^+ currents and the inward Ca^{2+} current (fig. 2c). Repolarization (phase 3) is achieved when the efflux of K^+ exceeds the influx of Ca^{2+}, and finally, the cell returns to the resting state (phase 4). During phases 0, 1, 2 and most part of phase 3 (up to the point where repolarization has reached about $-50\,\mathrm{mV}$) the cell is refractory to new current stimuli, i.e. it does not respond with another action potential. From this point forward, until it has become fully excitable, the cell is in the relative refractory period during which a new action potential can be evoked with stronger stimuli.

Figure 3 shows the APD restitution measured with an $S1-S2$ stimulus protocol (fig. 3a). The APD decreases as the DI shortens (fig. 3b). At very short DI the restitution curve is steep, with a slope > 1. If the diastolic interval is less than a critical value, the $S2$ stimulus falls within the refractory period of the $S1$ action potential and a new AP cannot be elicited.

Next, we periodically paced the cardiac fiber at $x = 0$ with a square-wave stimulus ($I_{stim} = \frac{\mu\mathrm{A}}{\mathrm{cm}^2}$, duration 2 ms) at four different frequencies. Figure 4 shows action potential traces from 40 positions along the cable. At 1.6 Hz, the cable responds with an action potential to every stimulus, resulting in a $\{1:1\}$ synchronization (fig. 4a), which would correspond to normal sinus rhythm. Increasing the stimulus frequency to 3.6 Hz results again in a $\{1:1\}$ rhythm (fig. 4b), however concordant alternans starts to develop. At a slightly higher frequency of 3.8 Hz, the cable responds with $\{2:1\}$ synchronization and transition to $\{2:2\}$ rhythm (fig. 4c). Finally, at 4.3 Hz the cable responds with an action potential at every other stimulus, resulting in a $\{2:1\}$ electrical rhythm.

To illustrate the onset of discordant alternans we followed the approach described in [10]. An ectopic stimulus was delivered at the top end of the cable (black arrow in fig. 5a) short after a sinus wave has finished traveling up the cable (shown at the left edge in fig. 5a). Sinus rhythm stimuli were thereafter given at 240 ms intervals

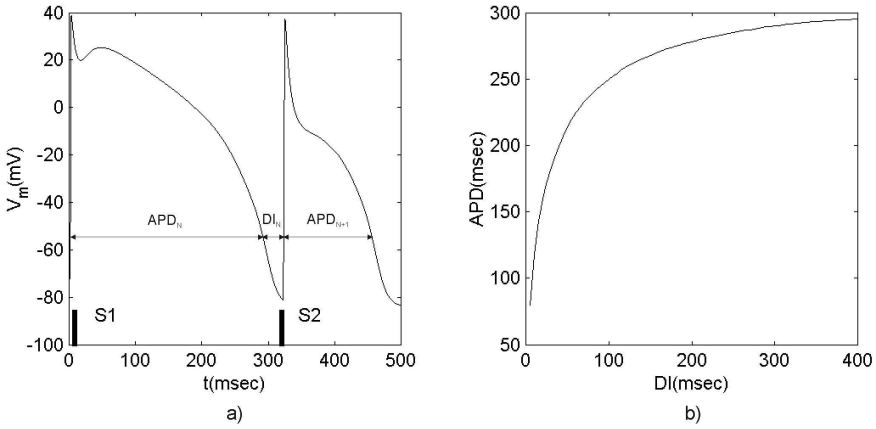

Fig. 3. Illustration of the APD restitution property of cardiac cells: a) action potentials resulted from a $S1 - S2$ stimulus protocol corresponding to a diastolic interval $DI = 5\,\text{ms}$ ($S1$ and $S2$ stimuli are shown with bars); b) restitution curve $APD_{N+1} = f(DI_N)$. Action potential duration APD_{N+1} elicited by the $S2$ stimulus decreases with the decrease of the previous diastolic interval DI_N.

at the bottom end of the cable. The periodic pacing produced discordant alternans, with short-long-short APD at the bottom end and long-short-long APD at the top end of the cable. The development of discordant alternans is strongly dependent on the coupling interval of the ectopic beat and the frequency of the sinus excitations. At lower sinus rates, only concordant alternans were seen. Figure 5b illustrates the same scenario in the case where the magnitude of the Ca^{2+} current was reduced by 25%. In this situation, the sinus excitations did not result in discordant nor in concordant alternans, and produced a $\{1:1\}$ periodic rhythm with a shorter APD.

4. Conclusions

In this study we used an electrophysiologic model of the cardiac cell and the cable equation to simulate electrical rhythms in a paced one-dimensional cardiac fiber. Our results show complex patterns of action potential propagation, determined mainly by the APD restitution properties of the cardiac tissue. The response of the cardiac fiber varies with the frequency of the stimulus train. High rate pacing leads to the development of concordant alternans.

Strong oscillations of APD were noted at around 3.6 Hz. Conduction block and $\{2:1 \rightarrow 2:2\}$ transition were observed at 3.8 Hz. Further increasing the frequency resulted in a $\{2:1\}$ electrical rhythm.

Discordant alternans were induced by delivering an ectopic stimulus during a fast rate sinus rhythm. During discordant alternans the APD shows a long-short-long pattern at one end of the cable and a short-long-short pattern at the other end. When

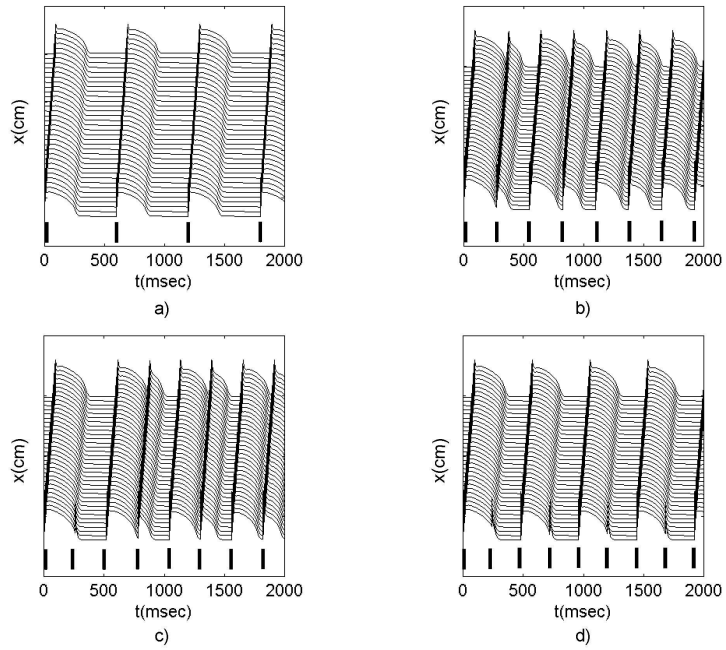

Fig. 4. Space-time diagrams of action potential propagation in a 7 cm cable paced at the bottom-end with a train of short current pulses at different frequencies. The stimulus train is shown with bars. a) at 1.6 Hz the cable responds with an action potential for every stimulus ($\{1:1\}$ rhythm); b) concordant alternans starts to develop at 3.6 Hz; c) at 3.8 Hz the cable has first a $\{2:1\}$ rhythm followed by a transition to $\{2:2\}$ rhythms; d) at 4.3 Hz there is a $\{2:1\}$ synchronization in which the cable responds with an action potential only to every other stimulus.

the magnitude of the calcium current I_S was reduced by 25%, neither concordant alternans nor discordant alternans occurred. The action potential was shortened, resulting in a prolongation of the diastolic interval. Although calcium channel blockers are used clinically to suppress alternans and other cardiac arrhythmias, they suffer from diminishing the contractile force of the ventricle by reducing the APD.

Our approach is computational only, and it only surfaces the complex behavior of cardiac tissue under normal and abnormal conditions. Nonetheless, the results presented suggest that computer models based on a detailed formulation of electrophysiologic processes may have the ability to accurately simulate complex responses of cardiac cells and may facilitate the development of pharmacological approaches to eliminating cardiac arrhythmias.

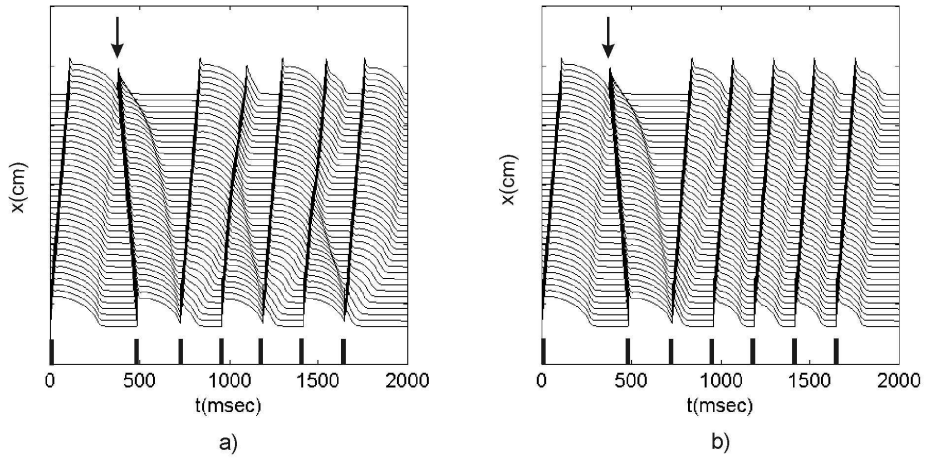

Fig. 5. Space-time diagram of action potential propagation in a 7 cm cable: a) discordant APD alternans were produced by delivering an ectopic stimulus (shown with arrow) at the top end of the cable followed by a high-rate pacing at the bottom end of the cable (240ms between stimuli); b) APD alternans were suppressed by reducing the Ca^{2+} current, I_S, by 25%.

References

[1] R.M. Berne, M.N. Levy, B.M. Koeppen et al., *Physiology*, Mosby Inc. Fourth Edition, 1998.

[2] D.R. Chialvo, R.F. Gilmour, J. Jalife, *Low dimensional chaos in cardiac tissue*, Nature, **343** (1990), 653–657.

[3] J.M. Pastore, S.D. Girouard, K.R. Laurita et al., *Mechanism linking T-wave alternans to the genesis of cardiac fibrillation*, Cir. Res., **99** (1999), 1385–1394.

[4] Z. Qu, J.N. Weiss, A. Garfinkel, *Cardiac electrical restitution properties and stability of reentrant spiral waves: a simulation study*, Am. J. Physiol., **276** (1999), 268–263.

[5] M.R. Guevara, G. Ward, A. Shrier, L. Glass, *Electrical alternans and period doubling bifurcations*, IEEE Comp. Cardiol., **562** (1984), 167–170.

[6] G.W. Beeler, H. Reuter, *Reconstruction of the action potential of ventricular myocardial fibres*, J. Physiol., **268** (1977), 177–210.

[7] T.F. Weiss, *Cellular Biophysics*, The MIT Press, Cambridge MA, 1996.

[8] J.P. Drouhard, F.A. Roberge, *Revised formulation of the Hodgkin-Huxley representation of the sodium current in cardiac cells*, Comp. Biomed. Res., **20** (1987), 333–350.

[9] A.M. Morega, *Modelare numerică pentru probleme la limită în inginerie*, MatrixRom, Bucureşti, 1998.

[10] M.A. Watanabe, F.H. Fenton, S.J. Evans et al., *Mechanisms for discordant alternans*, J. Cardiovasc. Electrophysiol, **12** (2001), 196–206.

[11] J.J. Fox, J.L. McHarg, R.F. Gilmour, *Ionic mechanism of electrical alternans*, Am. J. Physiol. Circ. Physiol., **282** (2002), H516–H530.

[12] A. Garfinkel, Y.H. Kim, O. Voroshilovsky et al., *Preventing ventricular fibrillation by flattening cardiac restitution*, Proc. Natl. Acad. Sci. USA, **97** (2000), 6061–6066.